

# Synthesis, Structure, and Catalytic Reactivity of Isolated V<sup>5+</sup>-Oxo Species Prepared by Sublimation of VOCl<sub>3</sub> onto H-ZSM5

Howard S. Lacheen and Enrique Iglesia\*

Department of Chemical Engineering, University of California at Berkeley, Berkeley, California 94720

Received: September 26, 2005; In Final Form: December 1, 2005

Isolated and uniform V<sup>5+</sup>-oxo species were grafted onto H-ZSM5 at V/Al<sub>f</sub> ratios of 0.2–1 via sublimation of VOCl<sub>3</sub> precursors. These methods avoid the restricted diffusion of solvated oligomers in aqueous exchange, which leads to poorly dispersed V<sub>2</sub>O<sub>5</sub> at external zeolite surfaces. Sublimation methods led to stable and active V-ZSM5 catalysts for oxidative dehydrogenation (ODH) reactions; they led to an order of magnitude increase in primary C<sub>2</sub>H<sub>6</sub> ODH rates compared with impregnated ZSM5 catalysts at similar V/Al<sub>f</sub> ratios and showed similar activity to impregnated VO<sub>x</sub>/Al<sub>2</sub>O<sub>3</sub>. The structure of grafted V<sup>5+</sup>-oxo species was probed using spectroscopic and titration methods. Infrared spectra in the OH region and isotopic exchange of D<sub>2</sub> with residual OH groups showed that exposure to VOCl<sub>3(g)</sub> at 473 K led to stoichiometric replacement of H<sup>+</sup> by each (VOCl<sub>2</sub>)<sup>+</sup> species. Raman spectra supported by Density Functional Theory electronic structure and frequency calculations showed that, at V/Al<sub>f</sub> < 0.5, hydrolysis and subsequent dehydration led to the predominant formation of (VO<sub>2</sub>)<sup>+</sup> species coordinated to one Al site with single-site catalytic behavior (0.7–0.9 × 10<sup>-3</sup> mol C<sub>2</sub>H<sub>4</sub> V<sup>-1</sup> s<sup>-1</sup>, 673 K). At higher V/Al<sub>f</sub> ratios, simulation of extended X-ray absorption fine structure spectra indicated that V<sub>2</sub>O<sub>4</sub><sup>2+</sup> dimers coexisted with VO<sub>2</sub><sup>+</sup> monomers and led to an enhancement in ODH rates as a result of bridging V–O–V (1.3 × 10<sup>-3</sup> mol C<sub>2</sub>H<sub>4</sub> V<sup>-1</sup> s<sup>-1</sup>). These V<sup>5+</sup>-oxo species form via initial reactions between VOCl<sub>3(g)</sub> and OH groups to form HCl<sub>(g)</sub>, hydrolysis of grafted (VOCl<sub>2</sub>)<sup>+</sup> to form HCl<sub>(g)</sub> and (VO(OH)<sub>2</sub>)<sup>+</sup>, and intramolecular and intermolecular condensation to form monomers and dimers, respective with the concurrent evolution of H<sub>2</sub>O. Raman and X-ray spectroscopies did not detect crystalline V<sub>2</sub>O<sub>5</sub> at V/Al<sub>f</sub> ratios of 0.2–1, but V<sub>2</sub>O<sub>5</sub> crystals were apparent in samples prepared by impregnation or physical mixtures of V<sub>2</sub>O<sub>5</sub>/H-ZSM5. Framework Al atoms and zeolite crystal structures are maintained during VOCl<sub>3</sub> treatment and subsequent hydrolysis; <sup>27</sup>Al and <sup>29</sup>Si MAS NMR showed that these synthetic protocols removes <10% of the framework Al atoms (Al<sub>f</sub>).

## 1. Introduction

The formation of stable single-site catalytic materials, for which the structure and function of active sites do not depend on the number density of active sites, can simplify the elucidation of reaction mechanisms and of the structures required for catalysis, and lead to higher and more predictable rates and selectivities. Here, we describe the synthesis and structure of isolated V<sup>5+</sup>-oxo species within medium-pore zeolites and probe structure–function relations for the oxidative dehydrogenation of C<sub>2</sub>H<sub>6</sub>.

Several studies have addressed the hydrothermal and post-synthesis exchange of V<sup>5+</sup>-oxo species into the zeolite lattice in medium and large-pore aluminosilicates.<sup>1–10</sup> Exchange of high-valent metal-oxo species from aqueous solutions into cationic exchange sites is limited by the large size and multiple charge of solvated isopolyanion clusters in aqueous media, which impair diffusion within zeolite channels, at pH levels consistent with stable aluminosilicate frameworks.<sup>11</sup> Exchange from V<sub>2</sub>O<sub>5</sub> crystallites in physical mixtures was claimed for Y-zeolite (0.76 nm window size),<sup>12</sup> but similar protocols led to V<sub>2</sub>O<sub>5</sub> structures at external surfaces for medium-pore zeolites (<0.6 nm channels).<sup>13</sup> V<sub>2</sub>O<sub>5</sub> is a nonvolatile compound with distorted trigonal bipyramidal symmetry, which cannot enter

10-ring channels (e.g., in ZSM5), even after melting (at 963 K). Physical mixtures of V<sub>2</sub>O<sub>5</sub> and H-ZSM5 were also proposed to form tetrahedral (≡SiO)<sub>3</sub>≡V=O species via reactions with external silanols (≡Si–OH) during treatment of V<sub>2</sub>O<sub>5</sub>/ZSM5 physical mixtures in air at 1023 K; such materials were active for photocatalytic *cis*-2-butene isomerization.<sup>9,14</sup>

Whittington, et al.<sup>15</sup> reported toluene oxidation catalysts prepared by contact of H-ZSM5 with VOCl<sub>3</sub> vapor at 593–793 K, a procedure that led to the removal of most infrared bands for both acidic and silanol OH groups and to extensive zeolite dealumination, but evidence for exchange or for the structure of the resulting VO<sub>x</sub> species was not provided. V-ZSM5, prepared via either impregnation or sublimation methods, catalyzes oxidative C<sub>2</sub>H<sub>6</sub> dehydrogenation; the higher reactivity of impregnated samples was attributed to the prevalence of residual acid sites, which also led to combustion side reactions,<sup>16</sup> as shown by others.<sup>17</sup> The latter study, however, reported higher oxidative dehydrogenation (ODH) rates on V-ZSM5 prepared by VOCl<sub>3</sub> than on H-ZSM5. These higher rates were proposed to reflect the formation of defect sites by incorporation of V<sup>5+</sup> into the zeolite framework during sublimation.

Recently, we have shown that V-ZSM5 samples prepared via sublimation of VOCl<sub>3</sub> onto H-ZSM5 catalyzes the selective pyrolysis of CH<sub>4</sub> to arenes at 973 K,<sup>18</sup> a finding that led to the systematic study of synthetic protocols and resulting structures

\* To whom correspondence should be addressed; iglesias@chem.berkeley.edu.

reported here. We provide evidence for the structure and exchange stoichiometry of V<sup>5+</sup>-oxo species formed via reaction of VOCl<sub>3(g)</sub> with acidic OH groups in H-ZSM5 at V/Al<sub>f</sub> atomic ratios up to unity (Al<sub>f</sub>, framework Al atoms). Spectroscopic and site titration methods indicate the presence of isolated vanadia structures at all V contents. The essential absence of silanols in these samples and the low temperatures (473 K) used for grafting VOCl<sub>3</sub> precursors avoided extensive dealumination and the formation of nonuniform structures prevalent in previous reports.

In this study, we also show how complementary techniques are required for unequivocal structural assessments of dispersed metal-oxo species and how the mere contact of microporous solids with aqueous or solid precursors is a nonrigorous and often inaccurate definition of exchange, except when serendipitous sublimation of extracrystalline debris causes inadvertent exchange during subsequent thermal treatments. Finally, we report catalytic rates of C<sub>2</sub>H<sub>6</sub> ODH on V-ZSM5 prepared by VOCl<sub>3</sub> sublimation as a function of V content; these rates are higher than those on isolated vanadyls on Al<sub>2</sub>O<sub>3</sub> and on VO<sub>x</sub> structures prepared by impregnation of H-ZSM5 with vanadium precursors.

## 2. Experimental Apparatus and Procedure

**2.1. Synthesis of Exchanged V-ZSM5.** H-ZSM5 was prepared by heating NH<sub>4</sub>-ZSM5 (7–8 g; AlSiPenta, Si/Al = 12.5; <0.03 wt % Na) to 623 K at 0.05 K s<sup>-1</sup> in dry air (1.67 cm<sup>3</sup> s<sup>-1</sup> g<sup>-1</sup>, Airgas, 99.999%) and held at 623 K for 3 h to remove physisorbed H<sub>2</sub>O. The zeolite was then heated to 773 K at 0.017 K s<sup>-1</sup> and held at 773 K for 5 h to convert NH<sub>4</sub>-ZSM5 into H-ZSM5. <sup>27</sup>Al MAS NMR spectra were collected on H-ZSM5 after thermal treatment (probe and method described in Section 2.2). These samples contained approximately 90% of their Al atoms in tetrahedral framework positions (Al<sub>f</sub>), corresponding to a Si/Al<sub>f</sub> ratio of 13.4. Na-ZSM5 was prepared by exchanging NH<sub>4</sub>-ZSM5 (1 g) twice with fresh 1 M NaCl<sub>(aq)</sub> (2 L) at 353 K for 12 h. Zeolites were washed with 2 L deionized doubly distilled H<sub>2</sub>O after removing the liquids from exchanged products by filtration.

V-ZSM5 was prepared from VOCl<sub>3</sub> and H-ZSM5 using an anhydrous vapor exchange process.<sup>18</sup> H-ZSM5 (2 g) was dehydrated in a vacuum (<0.13 Pa) within a sublimation reactor (shown in Figure 1) at 573 K for 3.6 ks. The reactor valve (*a*, Figure 1) was then closed and the reactor transferred to a N<sub>2</sub> atmosphere in which liquid VOCl<sub>3</sub> was injected, by syringe, into the reactor at *b*. Direct contact between liquid and zeolite was prevented using a cup within the sublimation reactor. After injecting VOCl<sub>3</sub>, the reactor was evacuated again and sealed at the neck *c* to form an ampule. This ampule was cooled to 200 K during reevacuation to prevent evaporative loss of VOCl<sub>3</sub> into the vacuum lines. The sealed ampule was then heated to 473 K for 5 h. The contents of the ampule (in 0.2–0.5 g batches) were transferred into a fritted quartz U-tube reactor heated to 473 K at 0.017 K s<sup>-1</sup> in 1 cm<sup>3</sup> s<sup>-1</sup> He (Praxair, 99.999%). The flow was then switched to a mixture of O<sub>2</sub> (20 kPa) and H<sub>2</sub>O (0.5 kPa) with He (81 kPa) as the balance by passing a stream of 1 cm<sup>3</sup> s<sup>-1</sup> 20% O<sub>2</sub>/He (Praxair, 99.999%) through a bubbler held at 273 K. After 7.2 ks, the bubbler was bypassed and the reactor was heated to 773 K at 0.017 K s<sup>-1</sup> for 3.6 ks. Finally, V-ZSM5 samples were cooled to ambient temperature and stored in a drybox until further analysis (described in Section 2.2). The number of framework Al atoms decreased slightly after exchange in most V-ZSM5 samples; therefore, V contents are reported throughout as the ratio of V atoms to framework Al atoms in the parent H-ZSM5 (V/Al<sub>f,i</sub>) or by V atoms to

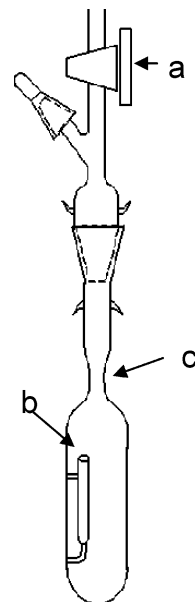


**Figure 1.** Schematic of borosilicate glass cell for sublimation and vapor-exchange of VO<sub>x</sub> precursors.

**TABLE 1: V<sup>5+</sup> Solutions (0.5 L) Used for Preparation of V-ZSM5**

solution no.	method <sup>a</sup>	V <sup>5+</sup> molarity (mM)	pH	aqueous V <sup>5+</sup> species	H-ZSM5 (g)
1	AE	0.06	4	VO <sub>2</sub> (OH) <sub>2</sub> <sup>-</sup>	0.2
2	AE	0.9	2.8	VO <sub>2</sub> <sup>+</sup>	0.2
3	AE	6	5	V <sub>10</sub> O <sub>27</sub> (OH) <sup>5-</sup>	0.24
4	Imp.	300	6.2	V <sub>10</sub> O <sub>28</sub> <sup>6-</sup>	0.2

<sup>a</sup> AE, aqueous exchange at 353 K for 12 h; Imp., wet impregnation.

framework Al in V-ZSM5, with the framework Al content determined by <sup>27</sup>Al MAS NMR (V/Al<sub>f,i</sub>) for each sample.

Samples were also prepared using aqueous vanadium precursors and either aqueous exchange or wet impregnation protocols. In the former, three solutions were prepared with varying pH and vanadium concentration. The solutions used for all materials, prepared from aqueous media and the V<sup>5+</sup> isopolyanion or cation structures prevalent at such conditions,<sup>19</sup> are given in Table 1.

**2.2. Structural and Chemical Characterization of V-ZSM5.** Residual protons in H-ZSM5 were measured by treating V-ZSM5 (0.2 g) samples with 5% D<sub>2</sub>/Ar (Matheson, 99.999%) at 1 cm<sup>3</sup> s<sup>-1</sup> total flow and heating to 873 K at 0.17 K s<sup>-1</sup>.<sup>20</sup> The effluent H<sub>2</sub> (2 amu), HD (3 amu), and D<sub>2</sub> (4 amu) concentrations were measured by mass spectrometry (MKS Minilab) using a differentially pumped atmospheric sampling system and heated (423 K) transfer lines. Flow rates and response factors were calculated using Ar (36 amu for <sup>36</sup>Ar, 0.34% natural abundance, because of a saturated signal at 40 amu) as an internal standard. The HD response factor was estimated as the geometric mean of the response factors for H<sub>2</sub> and D<sub>2</sub>; it was confirmed by equilibrating equimolar H<sub>2</sub>/D<sub>2</sub> mixtures on 1.5 wt. % Pt/ZrO<sub>2</sub> at 673 K.

V-ZSM5 samples were pressed into wafers for Raman spectroscopy studies and heated ex situ in dry air (Praxair, 99.999%) to 1023 K at 0.17 K s<sup>-1</sup> and held for 0.1 h. This procedure removed adsorbed unsaturated hydrocarbons, which fluoresce strongly and decrease Raman band intensities.<sup>21</sup> Wafers were heated to 823 K at 0.17 K s<sup>-1</sup> in dry air and held for 1 h to remove physisorbed H<sub>2</sub>O; they were then cooled to ambient temperature before measuring spectra using a rotating cell (~7 Hz) that minimizes sample damage by laser heating.

Spectra were recorded with a HoloLab 5000 research raman spectrometer (Kaiser Optical Systems, Inc.) using a 532 nm laser.

Infrared spectra were measured in transmission mode using a Mattson Research Series 10000 Fourier transform spectrometer. Wafers (15 mg cm<sup>-2</sup>) were treated at 673 K in dry air (Praxair, 99.999%) for 1 h within a cell sealed hermetically by CaF<sub>2</sub> windows. Spectra were recorded at 673 K with 2 cm<sup>-1</sup> resolution using 1000 scans. All bands were normalized by the intensity of framework overtone bands (1730–2100 cm<sup>-1</sup>) for ZSM5.

<sup>29</sup>Si and <sup>27</sup>Al nuclear magnetic resonance spectra were measured with magic angle spinning (MAS NMR) using a Bruker AV-500 (11.7T) spectrometer. <sup>29</sup>Si NMR were recorded at 99.3 MHz with a spinning rate of 10 kHz using a single 40° pulse (1.8 μs), a 2 s delay, 2000 scans, and a sweep width of 50 kHz. <sup>27</sup>Al NMR were recorded at 130.3 MHz with a spinning rate of 14 kHz using a single 9° pulse (1.22 μs), 1 s recycle delay, 3600 scans, and a sweep width of 500 kHz. Chemical shifts are reported relative to tetramethylsilane (TMS) for <sup>29</sup>Si and 1 M Al(NO<sub>3</sub>)<sub>3(aq)</sub> for <sup>27</sup>Al. Si/Al<sub>f</sub> ratios were estimated from <sup>29</sup>Si MAS NMR using integrated intensities, *I<sub>n</sub>*, for each Q<sup>4</sup>(nAl)<sup>22</sup> site and eq 1.<sup>23</sup> X-ray absorption spectra were

$$\frac{\text{Si}}{\text{Al}_f} = \frac{I_0 + I_1 + I_2 + I_3 + I_4}{0.25I_1 + 0.5I_2 + 0.75I_3 + I_4} \quad (1)$$

measured at the Stanford Synchrotron Radiation Laboratory using beamlines 2–3 and 6–2. Spectra were recorded in transmission mode using three ionization chambers in series filled with a constant N<sub>2</sub> flow. Catalyst samples were pressed into pellets and placed within a flow cell held between the first two detectors; a V-metal foil (2.5 μm) was inserted between the last two detectors. Energies were calibrated using the first inflection point in the V foil K-edge (5.465 keV). The beamline was equipped with a Si(111) double-crystal monochromator and a downstream horizontal aperture (0.2 mm × 5.0 mm). Signal intensities were detuned to 50% of their maximum values to minimize harmonics.

Spectra were analyzed using WinXAS Version 2.1<sup>24</sup> by subtracting pre-edge and post-edge backgrounds using first-order and third-order polynomials, respectively. The spectra were transformed between 0.35 and 1.8 nm<sup>-1</sup> in k-space. Back-transformed Fourier transformed (FT) EXAFS (0.1–0.4 nm, Bessel window) were fit using FEFFIT<sup>25</sup> software to determine interatomic distances (*R*), coordination numbers (*CN*), and Debye–Waller factors (*σ*<sup>2</sup>).<sup>26,27</sup> Fits were performed on *k*<sup>1</sup>- and *k*<sup>3</sup>-weighed extended fine structure spectra (EXAFS). Correlations between *CN* and *σ*<sup>2</sup> and between *R* and  $\Delta E_0$  values were decoupled by varying the *k*-weighing in the regression analysis.<sup>28</sup> Theoretical backscattering amplitude and phase shift functions were generated using FEFF8.2.<sup>29</sup> ATOMS<sup>30</sup> was used to generate the FEFF input files from previously reported atomic coordinates or from density functional theory (DFT) simulations. The amplitude reduction factor, *S<sub>0</sub>*<sup>2</sup>, was determined by fitting experimental spectra for crystalline V<sub>2</sub>O<sub>5</sub>.

**2.3. Density Functional Theory Calculations.** Density functional theory was used to assess potential VO<sub>x</sub> structures grafted onto H-ZSM5 structures by estimating bond lengths and angles and the vibrational spectra of possible V-oxo species. Calculations were performed using Gaussian 03 Rev. B.04<sup>31</sup> with a local spin density approximation (S-VWN5)<sup>32,33</sup> and also with Becke's hybrid exchange functional, which includes a mixture of Hartree–Fock exchange with DFT exchange–

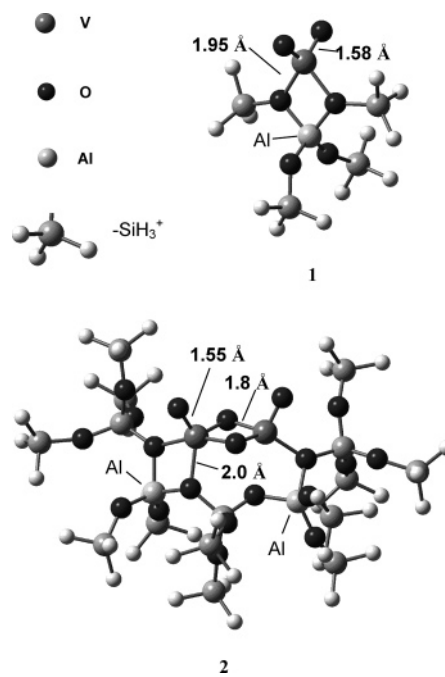


**Figure 2.** Relaxed VO<sub>2</sub><sup>+</sup> and V<sub>2</sub>O<sub>4</sub><sup>2+</sup> structures in H-ZSM5 using B3LYP/6-31G(d) and Gaussian 03. SiH<sub>3</sub><sup>+</sup> groups were fixed in position to maintain ZSM5 structure during optimization.

correlation, with the Lee, Yang, and Parr correlation functional (B3LYP).<sup>34,35</sup> The 6-31G(d)<sup>36</sup> basis set with polarization functions added to all atoms, except terminal hydrogen atoms, was used to minimize electronic energies. The starting point for the zeolite framework used for VO<sub>2</sub><sup>+</sup> structures was the set of crystallographic coordinates for T-12<sup>37,38</sup> sites in a 5T silicalite-1 cluster (Figure 2, Structure 1). This T-12 site was replaced by an Al atom bonded through oxygen atoms to four silicon atoms terminated with hydrogen atoms. Fully relaxed simulations on smaller VO<sub>2</sub>(OH)<sub>2</sub>Al(OH)<sub>2</sub> clusters were also performed to verify structures and frequencies in larger constrained VO<sub>2</sub><sup>+</sup>-ZSM5 structures. For V<sub>2</sub>O<sub>4</sub><sup>2+</sup> dimers, the starting point was a 17T ZSM5 cluster with two next-nearest neighboring T-sites replaced by Al atoms (Structure 2). The V<sub>2</sub>O<sub>4</sub><sup>2+</sup> dimers were placed in a segment of a ten-membered ring consisting of seven T-sites. All Si and H atoms were fixed.

Raman-active modes were obtained from the calculated vibrational spectra of optimized structures using Gaussian 03. DFT methods overestimate stretching frequencies because of systematic inaccuracies in calculations of second derivatives for potential energy surfaces, electronic correlations, and the harmonic approximation.<sup>39–41</sup> An average scaling factor was used to correct calculated frequencies for comparison with experiments; scaling factors of 0.9613 and 0.9833 have been recommended for the B3LYP/6-31G(d) and S-VWN5/6-31G(d) combination, respectively.<sup>41</sup> We estimate the accuracy of the estimates for vibrational frequencies to be ± 20 cm<sup>-1</sup>.<sup>42</sup>

**2.4. Oxidative Dehydrogenation of C<sub>2</sub>H<sub>6</sub>.** Ethane ODH rates were measured in a quartz flow reactor using 0.05–0.10 g catalyst at 673 K, 14 kPa C<sub>2</sub>H<sub>6</sub> (Airgas, 99.999%), 1.7 kPa O<sub>2</sub> (Airgas, 99.999%), and He as the balance (Praxair, 99.999%). Space velocities were varied to achieve ethane conversions of 0.5–2.5% and to estimate pseudo-first-order rate constants for ODH (*k*<sub>1</sub>) and for combustion of C<sub>2</sub>H<sub>6</sub> (*k*<sub>2</sub>) and C<sub>2</sub>H<sub>4</sub> (*k*<sub>3</sub>), using reported methods.<sup>43</sup> Effluent concentrations were measured by gas chromatography (Agilent 6890 GC) using a capillary column (HP-Plot Q) with flame ionization detection, and a packed column (Carboxen 1004) with thermal conductivity detection.

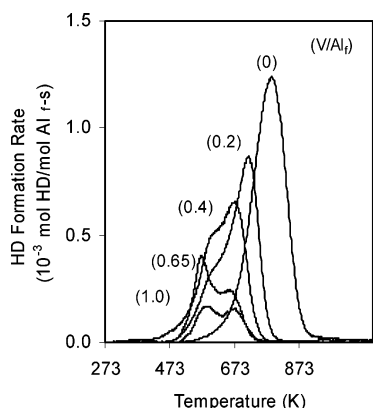


**Figure 3.** Formation rate of HD vs temperature on H-ZSM5 ( $\text{Si}/\text{Al}_{\text{f,i}} = 13.4$ ) and V-ZSM5 ( $\text{V}/\text{Al}_{\text{f,i}} = 0.2-1$ ) during treatment in 5 kPa  $\text{D}_2$ /balance Ar. Dehydrated samples were heated to 873 K at  $0.17 \text{ K s}^{-1}$  and held for 0.5 h.

**TABLE 2: Residual Si–OH–Al Groups Measured Using  $\text{D}_2$ –OH Exchange and Infrared Spectroscopy<sup>a</sup>**

$\text{V}/\text{Al}_{\text{f,i}}$	$\text{D}_2\text{OH}$			FTIR		$E_a$ (kJ/mol)	A ( $\text{s}^{-1}$ )
	$2\text{H}_2 +$ HD	$\Delta\text{OH}/\text{V}$	$\Delta\text{OH}_{\text{Vex}}/\text{V}$	$\Delta\text{O}/\text{V}$	$\Delta\text{OH}_{\text{Vex}}/\text{V}$		
0	1.07					89	220 000
0.2	0.82	1.25	1.08	0.95	0.78	70	68 000
0.4	0.63	1.10	1.05	0.90	0.85	65	45 000
0.65	0.32	1.15	-	0.77			
1.0	0.16	0.91	0.81	0.94	0.84		

<sup>a</sup> Activation energies and pre-exponential factors for  $\text{D}_2$ –OH exchange were estimated assuming the rate was first order in both  $\text{D}_2$  and OH. The change in hydroxyls per vanadium was calculated two ways: using the amount of framework Al in the unexchanged H-ZSM5 ( $\Delta\text{OH}/\text{V}$ ) and using the amount of framework Al after  $\text{VOCl}_3$  treatment and hydrolysis ( $\Delta\text{OH}_{\text{Vex}}/\text{V}$ ).

### 3. Results and Discussion

**3.1. V<sup>5+</sup> Exchange Stoichiometry in H-ZSM5.** The number of OH groups removed during grafting of  $\text{VOCl}_3$  onto H-ZSM5 was measured by isotopic titration of residual OH with  $\text{D}_2$ , which forms HD as a primary product and  $\text{H}_2$  via secondary exchange of HD with residual OH groups.<sup>20,44</sup> Cations and metal–oxo species at exchange sites decreased the number of OH groups; alternate methods involving titration with  $\text{NH}_3$  or organic bases are inaccurate because such titrants also coordinate to the grafted cations.

Since  $\text{D}_2$ –OH exchange methods do not differentiate between protons at acid sites and silanols, we attempted to quantify the amount of silanols by selectively titrating acidic protons. Prins et al.<sup>45</sup> reported incomplete proton exchange by  $\text{Cs}^+$  using  $^1\text{H}$  MAS NMR and found that  $\text{Cs}^+$  only exchanges with acidic  $\text{H}^+$ ;  $\text{Na}^+$  is used in the present study because it is smaller than  $\text{Cs}^+$  and would, therefore, interact with OH groups that may be inaccessible to  $\text{Cs}^+$ . Isotopic titration methods with  $\text{D}_2$  gave 1.07 OH per framework aluminum ( $\text{Al}_{\text{f,i}}$ ) atom for H-ZSM5. Na-ZSM5, which contains  $\text{Na}^+$  cations at bridging framework Al sites, has fewer OH groups as expected (0.09 OH/ $\text{Al}_{\text{f,i}}$ ; evidence for replacement of only acidic  $\text{H}^+$  with  $\text{Na}^+$  is shown later by infrared spectra).

HD formation rates on V-ZSM5 are shown as a function of temperature in Figure 3. The change in the concentration of OH groups (expressed in units of  $\Delta\text{OH}/\text{Al}_{\text{f,i}}$  or hydrogen per framework Al in the unexchanged H-ZSM5) depended linearly on V content (Table 2) for  $\text{V}/\text{Al}_{\text{f,i}}$  ratios of 0.2–1, indicating that each  $\text{VOCl}_3$  precursor replaced  $1.1 \pm 0.2$  OH groups in all samples.

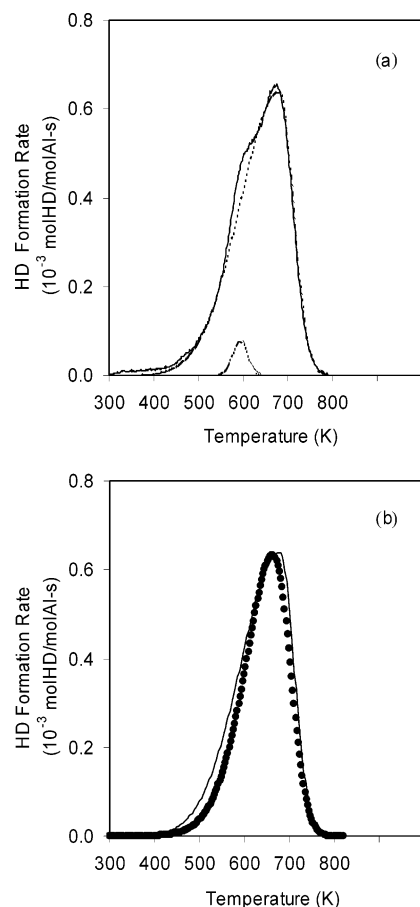


**Figure 4.** Formation rate of HD vs temperature on V-ZSM5 ( $\text{V}/\text{Al}_{\text{f,i}} = 0.4$ ) during treatment in 5 kPa  $\text{D}_2$ /balance Ar showing (a) deconvolution of HD formation rate and (b) fit of HD formation rate.

The maximum in HD formation rates decreased from 791 K in H-ZSM5 to 721 K for 0.2  $\text{V}/\text{Al}_{\text{f,i}}$  (V per framework Al in parent H-ZSM5 with  $\text{Si}/\text{Al}_{\text{f,i}} = 13.4$ ) and to 697 K for samples with  $\text{V}/\text{Al}_{\text{f,i}}$  ratios between 0.4 and 1.0. These trends reflect D–D dissociation and HD recombination catalyzed by V-oxo cations, as shown previously for  $\text{Zn}^{2+}$  and  $\text{Co}^{2+}$  in H-ZSM5.<sup>44,46</sup> V-ZSM5 samples also show a shoulder at 610 K. In samples with  $\text{V}/\text{Al}_{\text{f,i}}$  ratios of 0.4 or lower, this shoulder accounts for <5% of the O–H groups in the starting H-ZSM5 sample. These shoulders were subtracted using nonlinear regression methods with asymmetric Lorentzian functions to accurately determine the isotopic exchange dynamics corresponding to the high-temperature exchange process (Figure 4). Isotopic exchange rates were estimated by assuming that they depend linearly on the number of residual OH groups (eq 2; A, preexponential factor;  $E_a$ , activation energy for HD recombination).  $\text{D}_2$  is

$$\frac{d(\text{HD})}{dt} = -\frac{d(\text{OH})}{dt} = Ae^{-E_a/RT}[\text{D}_2][\text{OH}] \quad (2)$$

present in excess during  $\text{D}_2$ –OH, so HD dissociation rates depend only on temperature and  $[\text{OH}]$ . Equation 2 and the data in Figure 3 gave activation energies of  $\sim 65-70 \text{ kJ mol}^{-1}$  when H-ZSM5 was exchanged with  $\text{VOCl}_3$  and hydrolyzed (Table 2). The presence of extraframework cations effectively decreased  $E_a$  by 20–25  $\text{kJ mol}^{-1}$  in V-ZSM5 (from 89  $\text{kJ mol}^{-1}$  in H-ZSM5) resulting in the observed shift of the HD formation peak to lower temperatures.<sup>44,46</sup>

$\text{D}_2$ –OH measurements cannot distinguish between silanols and acidic hydroxyls; both undergo exchange at similar rates,

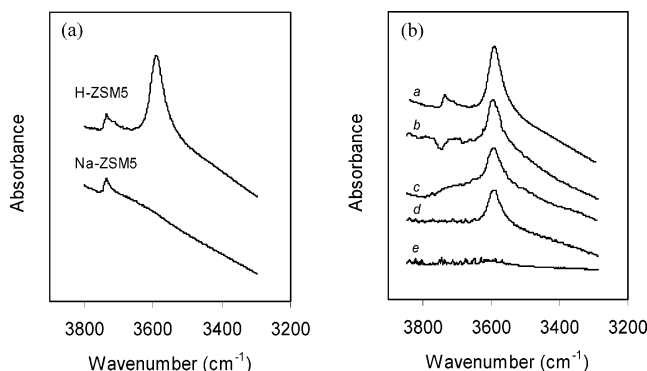


**Figure 5.** Fourier transformed infrared spectra in the hydroxyl stretching region of H-ZSM5 ( $\text{Si}/\text{Al}_{\text{f},i} = 13.4$ ), Na-ZSM5, and V-ZSM5 ( $\text{V}/\text{Al}_{\text{f},i} = 0.2\text{--}1.0$ ). In 5a, the spectra for H-ZSM5 and Na-ZSM5, prepared by aqueous exchange with NaCl, are shown. 5b shows (a) H-ZSM5, (b)  $\text{V}/\text{Al}_{\text{f},i} = 0.2$ , (c)  $\text{V}/\text{Al}_{\text{f},i} = 0.4$ , (d)  $\text{V}/\text{Al}_{\text{f},i} = 0.65$ , (e)  $\text{V}/\text{Al}_{\text{f},i} = 1$ . Spectral intensities were normalized by Si–O–Si overtone bands between 1730 and 2100  $\text{cm}^{-1}$ .

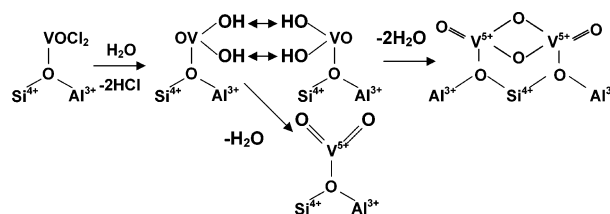
because exchange processes are limited by  $\text{D}_2$  dissociation steps;<sup>47</sup> therefore, here we use infrared spectra to measure the number of acidic OH groups removed during grafting of  $\text{VOCl}_3$  onto H-ZSM5. First, we measured the amounts of silanols and acidic hydroxyls in H-ZSM5. The O–H stretching region spectra for H-ZSM5 (Figure 5a) shows bands at 3600  $\text{cm}^{-1}$  for Si–OH–Al<sub>f</sub> groups and 3740  $\text{cm}^{-1}$  for silanols. Only silanol bands remain after two exchanges with  $\text{NaCl}_{(\text{aq})}$  (Figure 5a) because  $\text{Na}^+$  replaces only  $\text{H}^+$  at bridging Al<sub>f</sub> sites; nonacidic OH groups account for  $\sim 8\%$  of all OH groups in our H-ZSM5 sample, when calculated from the  $\text{OH}_{\text{NaZSM5}}/\text{OH}_{\text{HZSM5}}$  from  $\text{D}_2$ –OH exchange measurements.

The relative extinction coefficients for silanol and acidic hydroxyls were estimated to be within a factor of 2, using transmission infrared and  $\text{D}_2$ –OH measurements. Exact values could not be calculated as a result of the presence of a minority  $\text{Al}(\text{OH})_x$  band (3660  $\text{cm}^{-1}$ ) detected in Na-ZSM5 that overlapped silanol bands. In contrast, Kazansky et al.<sup>48</sup> reported extinction coefficients  $\sim 10$  times larger for acidic hydroxyls than for silanols using diffuse-reflectance methods and  $^1\text{H}$  MAS NMR spectra to determine the relative abundance of each OH group. The discrepancy between the two studies may arise from severe nonlinearities in diffuse reflectance spectra with pseudo-absorbances (given by the Kubelka-Monk formalism) above 10.

The intensity of Si–OH–Al bands decreased monotonically with increasing  $\text{V}/\text{Al}_{\text{f},i}$  ratio in V-ZSM5 prepared by sublimation of  $\text{VOCl}_3$  onto H-ZSM5. The change in the Si–OH–Al band (relative to that in unexchanged H-ZSM5, Figure 5b) corresponds to  $0.9 \pm 0.1$  OH replaced per V-atom (Table 2). This exchange stoichiometry is slightly lower than those measured from isotopic  $\text{D}_2$ –OH exchange ( $1.1 \pm 0.2$ ), because the latter includes V–O–Si groups formed by replacement of silanols.  $\text{VOCl}_3(\text{g})$  exchanges onto silanols in H-ZSM5 and silica below 593 K to form tetrahedral ( $\equiv\text{SiO})_3\text{V}=\text{O}$  species.<sup>15,49</sup> Infrared spectra of samples reported here (Figure 5b) confirmed that silanols also react with  $\text{VOCl}_3(\text{g})$  at 473 K to form such species, which account for  $<15\%$  of the V-atoms.

The required charge balance for  $\text{V}^{5+}$  centers and the exchange stoichiometry inferred from  $\text{D}_2$ –OH exchange and infrared spectra ( $\sim 1 \text{ V}/\text{Al}_{\text{f},i}$ ) are consistent with two possible V-oxo structures: (i)  $\text{VO}_2^+$  cations, isostructural with tetrahedral monovanadate ions ( $\text{VO}_4^{3-}$ ), at a single Al site, or (ii)  $\text{V}_2\text{O}_4^{2+}$  dimers with two  $\mu$ -oxo linkages and each V-atom interacting with an Al site via one V–O–Al linkage (Scheme 1). Al–O–

### SCHEME 1: Proposed V-ZSM5 Structures and Formation Pathway



Al linkages cannot exist in crystalline aluminosilicates; thus, dimers may form on next-nearest neighbor Al–Al pairs or with nonneighboring Al across a channel, the abundance of which is discussed in the next section.

$\text{D}_2$ –OH exchange and infrared methods do not probe vanadium-oxo structures directly, but measure instead residual OH groups; thus, they cannot provide definitive structural assignments for V-oxo species, which we attempt next using spectroscopic probes of the V valence and coordination in V-oxo species.

**3.2.  $^{27}\text{Al}$  and  $^{29}\text{Si}$  Nuclear Magnetic Resonance Spectroscopy.**  $^{27}\text{Al}$  MAS NMR spectra of V-ZSM5 samples show two types of Al centers (Figure 6a), one with a line at 55 ppm corresponding to framework T-sites ( $\text{Q}^{\text{tet}}$ ) and another one with a line at 0 ppm from extraframework octahedral Al centers ( $\text{Q}^{\text{oct}}$ ). The ratio of octahedral to tetrahedral Al centers in the starting H-ZSM5 (0.16) increased slightly (to 0.18–0.20) as  $\text{V}/\text{Al}_{\text{f},i}$  ratios increased from 0.2 to 0.4 and more noticeably (to 0.29) upon stoichiometric exchange of all centers ( $\text{V}/\text{Al}_{\text{f},i} = 1.0$ ) (Table 3). These changes in  $\text{Q}^{\text{tet}}/\text{Q}^{\text{oct}}$  ratios reflect the extraction of  $<10\%$  of the Al<sub>f</sub> centers in H-ZSM5 during exchange, probably during hydrolysis of  $\text{VOCl}_x\text{-ZSM5}$  at 473 K, which forms  $\text{HCl}_{(\text{g})}$  species that can extract framework Al as extraframework  $\text{AlCl}_3$ .

$^{29}\text{Si}$  MAS NMR showed two broad unresolved features at  $-107$  and  $-113$  ppm in H-ZSM5 (Figure 6), corresponding to  $\text{Q}^4(1\text{Al})$  and  $\text{Q}^4(0\text{Al})$  sites, respectively.<sup>22</sup> The small shoulder at  $-117$  ppm has been assigned also to  $\text{Q}^4(0\text{Al})$  species.<sup>50</sup>  $^{29}\text{Si}$  MAS NMR spectra for samples prepared by vapor exchange of  $\text{VOCl}_3$  and subsequent hydrolysis (Figure 6) are nearly identical to those for unexchanged H-ZSM5. The deconvolution of the spectra for the starting H-ZSM5 shows four lines ( $-117$ ,  $-113$ ,  $-107$ , and  $-103$  ppm); the first two lines are assigned

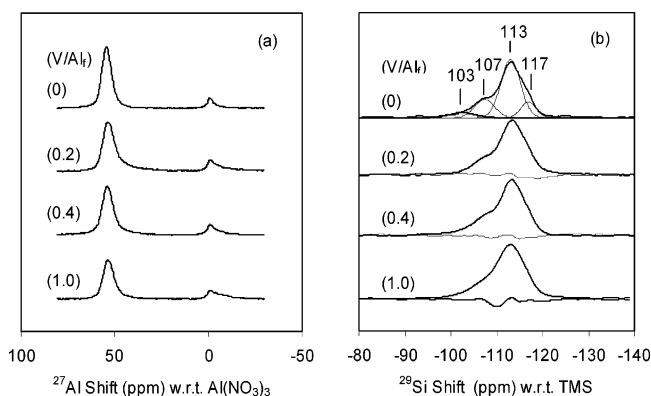


**Figure 6.** Solid-State NMR with magic angle spinning by (a) single pulse  $^{27}\text{Al}$  MAS NMR recorded at 11.7 T for H-ZSM5 ( $\text{Si}/\text{Al}_{\text{f},i} = 13.4$ ) and V-ZSM5 ( $\text{V}/\text{Al}_{\text{f},i} = 0.2\text{--}1.0$ ). Spectra are referenced to  $\text{Al}(\text{NO}_3)_3(\text{aq})$ . (b) Single pulse  $^{29}\text{Si}$  MAS NMR recorded at 11.7 T for H-ZSM5 ( $\text{Si}/\text{Al}_{\text{f},i} = 13.4$ ) and V-ZSM5 ( $\text{V}/\text{Al}_{\text{f},i} = 0.2\text{--}1$ ). Spectra are referenced to TMS. The difference between H-ZSM5 and V-ZSM5 is indicated below each  $^{29}\text{Si}$  spectra. Spectral deconvolution of  $\text{Q}^4(n\text{Al})$  sites is also shown for H-ZSM5 in (b).

**TABLE 3: Si/Al<sub>f</sub> Ratios and Relative Peak Areas in <sup>27</sup>Al and <sup>29</sup>Si MAS NMR Recorded at 11.7 T<sup>a</sup>**

V/Al <sub>f,i</sub>	<sup>27</sup> Al		<sup>29</sup> Si		% NNN Al <sub>f</sub>	Si/Al <sub>f</sub>
	Q <sup>oct</sup> /Q <sup>tet</sup>	Q <sup>4</sup> (1Al)/Q <sup>4</sup> (0Al)	Q <sup>4</sup> (2Al)/Q <sup>4</sup> (0Al)	Q <sup>4</sup> (1Al)/Q <sup>4</sup> (0Al)		
0	0.16	0.26	0.09	0.08	41	12.2
0.2	0.20	0.24	0.08	0.1	40	12.9
0.4	0.18	0.27	0.07	0.1	43	11.8
1.0	0.29	0.21	0.07	0.07	40	14.7

<sup>a</sup> Q<sup>tet</sup> and Q<sup>oct</sup> were Al species at 55 and 0 ppm relative to 1 M Al(NO<sub>3</sub>)<sub>3(aq)</sub>. Q<sup>4</sup>(*n*Al) areas were determined by deconvolution of <sup>29</sup>Si spectra allowing for Q<sup>4</sup>(0Al) full widths at half-height of maximum (FWHM) to vary 5% among samples. The Si/Al<sub>f</sub> ratio was calculated using eq 1. Percentages of next-nearest neighboring Al (% NNN Al<sub>f</sub>) were calculated by 2Q<sup>4</sup>(2Al)/[Q<sup>4</sup>(1Al)+2Q<sup>4</sup>(2Al)].

to Q<sup>4</sup>(0Al) Si atoms and the latter two to Q<sup>4</sup>(1Al) and Q<sup>4</sup>(2Al), respectively. The Si/Al<sub>f</sub> ratios estimated from these data using eq 1 are shown in Table 3. Unexchanged H-ZSM5 gives a Si/Al<sub>f</sub> ratio of 12.2, slightly smaller than that measured from <sup>27</sup>Al NMR (13.4), apparently because minority silanol Q<sup>3</sup> sites (Si(OH)(OSi)<sub>3</sub>) give chemical shifts similar to Q<sup>4</sup>(*n*Al). No detectable increase in Si/Al<sub>f</sub> was observed by <sup>29</sup>Si MAS NMR after exchange with VOCl<sub>3</sub> and subsequent hydrolysis.

The change in hydroxyls per V-atom can be estimated more rigorously by taking into account the number of OH groups lost by dealumination (from <sup>27</sup>Al MAS NMR) instead of exchange (Table 2, denoted as ΔOH<sub>Vex</sub>/V). In effect, here we renormalize the exchange stoichiometry to reflect only those hydroxyls removed by interactions with VOCl<sub>3(g)</sub>. Average exchange stoichiometries become 1.0 ± 0.2 for isotopic D<sub>2</sub>-OH exchange and 0.8 ± 0.1 from infrared spectra of acidic hydroxyls (Table 2).

The replacement of a single proton by each VOCl<sub>3</sub> species would be consistent with either the monomer or the dimer structures shown in Scheme 1. Typical V–O bond lengths and theoretical estimates of the size of V-oxo dimers using density functional theory (DFT, as also discussed in Section 3.4) indicate that V<sub>2</sub>O<sub>4</sub><sup>2+</sup> dimers would require Al–Al distances smaller than 0.85 nm. If framework Al atoms were randomly distributed, 57% of Al<sub>f</sub> centers would have another Al<sub>f</sub> within 0.85 nm in the same channel (for Si/Al<sub>f,i</sub> = 13.4; using calculations from Rice et al.).<sup>51</sup> Thus, dimers cannot be the only species formed for V/Al<sub>f,i</sub> ratios above ~0.5, while monomers, which require only a single Al atom, can form at all V/Al<sub>f,i</sub> ratios. Thus, at V/Al<sub>f,i</sub> ratios above 0.57, VO<sub>x</sub> monomers must be present, but we cannot rule out from these data the coexistence or even the predominance of dimers at lower V/Al<sub>f,i</sub> ratios. Next, we describe the use of X-ray absorption spectroscopy in an attempt to detect VO<sub>x</sub> monomers and dimers in V-ZSM5 samples prepared by grafting of VOCl<sub>3</sub> precursors.

**3.3. X-ray Absorption Spectroscopy.** Vanadium K-edge X-ray absorption spectra for physical mixtures of V<sub>2</sub>O<sub>5</sub> and H-ZSM5 treated in air at 973 K resemble that for crystalline V<sub>2</sub>O<sub>5</sub> (Figure 7), indicating that V<sub>2</sub>O<sub>5</sub> structures remain after thermal treatment. V-ZSM5 prepared by sublimation of VOCl<sub>3</sub> at 373 K, hydrolysis at 473 K, and thermal treatment in dry air at 773 K showed identical spectra for V/Al<sub>f</sub> ratios of 0.41 and 1.1, without detectable V<sub>2</sub>O<sub>5</sub> features.

Edge energies (the first inflection point after the pre-edge feature) relative to V metal showed that V-atoms are present as V<sup>5+</sup> in all V-ZSM5 samples prepared by grafting VOCl<sub>3</sub> (pre-edge not shown in Figure 7). VO<sub>2</sub> (13 ΔeV), V<sub>2</sub>O<sub>5</sub> (18.8 ΔeV), and V metal (0 ΔeV) gave a linear relationship between their edge-energies and oxidation states. V-ZSM5 samples gave absorption edge energies of 18.4 and 18.9 for V/Al<sub>f</sub> ratios of

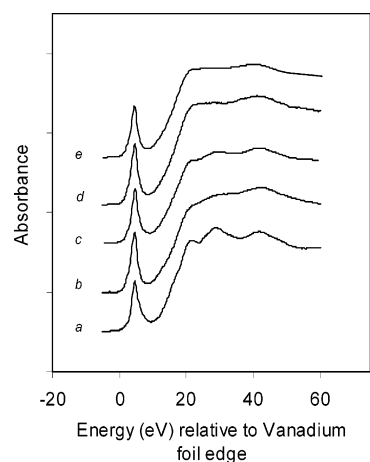


**Figure 7.** Vanadium K-edge near-edge spectra for (a) V<sub>2</sub>O<sub>5</sub>; V<sub>2</sub>O<sub>5</sub>/H-ZSM5 after thermal treatment in dry air at 973 K with V/Al<sub>f,i</sub> ratios of (b) 0.4 and (c) 1.0; V-ZSM5 prepared from VOCl<sub>3</sub> then hydrolyzed with V/Al<sub>f,i</sub> ratios of (d) 0.4 and (e) 1.0. Transmission spectra were recorded at 298 K.

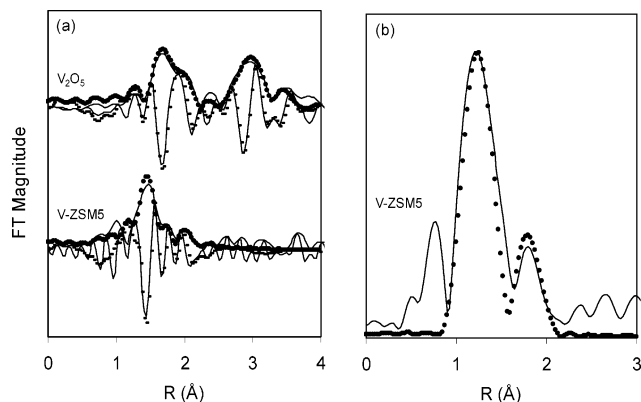


**Figure 8.** Fourier transformed *k*<sup>3</sup>-weighted EXAFS for V-ZSM5 (V/Al<sub>f,i</sub> = 1.0, 773 K) in 20% O<sub>2</sub>/He. Spectra were recorded at 298 K. (a) experimental magnitude and imaginary part of the phase corrected FT-EXAFS (—) and the fitted magnitude (···) and imaginary parts (---) using three V–O distances. (b) experimental magnitude of FT-AFS before phase correction (—) and the fit generated by varying the fraction of vanadium in VO<sub>2</sub><sup>+</sup> and V<sub>2</sub>O<sub>4</sub><sup>2+</sup> (···).

0.41 and 1.1, respectively, indicating that V remains pentavalent after VOCl<sub>3</sub> exchange, hydrolysis, and thermal treatment.

The phase-corrected radial scattering function obtained from the *k*<sup>3</sup>-weighed fine structure spectra for V<sub>2</sub>O<sub>5</sub> and V-ZSM5 (from VOCl<sub>3</sub> grafting; V/Al<sub>f</sub> = 1.1) showed strong features at 0.1–0.2 nm with a maximum at 0.15 nm (Figure 8).<sup>52</sup> Figure 8a shows the imaginary part of the fine structure for V<sub>2</sub>O<sub>5</sub> and for V-ZSM5 prepared by grafting of VOCl<sub>3</sub> precursors. The presence of one or multiple types of V–O scatterers in Figure 8a can be discerned by comparing the maximum of the imaginary component with that for the magnitude of the Fourier transformed spectrum. Maxima that occur at similar distances indicate the presence of only one type of oxygen atom.<sup>53</sup>

Crystalline V<sub>2</sub>O<sub>5</sub> has a distorted trigonal pyramidal structure and four distinct V–O distances (the V–O shell at 0.188 nm is doubly degenerate),<sup>54</sup> and the maxima do not coincide. The imaginary part and the magnitude of the radial scattering function are accurately described by incorporating all four V–O distances in the simulation (fitting parameters in Table 4). In V-ZSM5, the maxima also do not occur at the same radial position (Figure 8a), which led us to conclude that prevalent V-oxo structures have more than one type of oxygen scatterer around V centers. We used structures for VO<sub>2</sub><sup>+</sup> and V<sub>2</sub>O<sub>4</sub><sup>2+</sup>

**TABLE 4: Refined EXAFS Structural Parameters for V<sub>2</sub>O<sub>5</sub> and V-ZSM5 Prepared from VOCl<sub>3</sub> and Dehydrated at 773 K<sup>a</sup>**

shell	CN	predicted CN	R (nm, ± 2%)	predicted R (nm)	ΔE <sub>0</sub>	σ <sup>2</sup> (10 <sup>-5</sup> nm <sup>2</sup> , ± 50%)
V <sub>2</sub> O <sub>5</sub>						
O <sub>1</sub>	1 <sup>b</sup>	1	0.159	0.159	2.3	5
O <sub>2</sub>	1 <sup>b</sup>	1	0.181	0.178	2.3	0 <sup>b</sup>
O <sub>3</sub>	2 <sup>b</sup>	2	0.188	0.188	2.3	12
O <sub>4</sub>	1 <sup>b</sup>	1	0.198	0.202	2.3	0 <sup>b</sup>
O <sub>5</sub>	1 <sup>b</sup>	1	0.276	0.279	2.3	6
V <sub>1</sub>	2 <sup>b</sup>	2	0.310	0.309	4.6	5
V <sub>2</sub>	1 <sup>b</sup>	1	0.362	0.342	4.6	7
V-ZSM5 from VOCl <sub>3</sub> simulated with VO <sub>2</sub> <sup>+</sup>						
O <sub>1</sub>	0.8 ± 0.4	2	0.160	0.158	-7.6	1
O <sub>2</sub>	2 <sup>b</sup>	2	0.181	0.195	-7.6	18
V-ZSM5 from VOCl <sub>3</sub> simulated with V <sub>2</sub> O <sub>4</sub> <sup>2+</sup>						
O <sub>1</sub>	1.4 ± 0.6	1	0.160	0.155	-1	2
O <sub>2</sub>	2.7 ± 1.3	2	0.182	0.180	-1	11
O <sub>3</sub>	0.5 ± 0.2	2	0.202 <sup>b</sup>	0.202	-1	0 <sup>b</sup>
VO <sub>2</sub> <sup>+</sup> /V <sub>2</sub> O <sub>4</sub> <sup>2+</sup> binary mixture						

64% V in VO<sub>2</sub><sup>+</sup>/36% V in V<sub>2</sub>O<sub>4</sub><sup>2+</sup> (±15%)

<sup>a</sup> Spectra were recorded at 298 K and fit using 1 spectra for V<sub>2</sub>O<sub>5</sub> and 12 averaged spectra for V-ZSM5. Fitting was performed on k<sup>3</sup> weighted spectra. Refined value of S<sub>0</sub><sup>2</sup> was 0.84. <sup>b</sup> Fixed.

cations from DFT simulations (Figure 2) as starting points to describe these radial structure functions. The three V–O distances in V<sub>2</sub>O<sub>4</sub><sup>2+</sup> gave better fits than the two V–O distances in VO<sub>2</sub><sup>+</sup>; the fitted V–O shells are at 0.160, 0.182, and 0.202 nm, in agreement with the simulated dimer structure (Table 4). Coordination numbers for these V–O shells, however, were not consistent with dimer structures within experimental error. The EXAFS spectra for V-ZSM5 was reanalyzed by varying only the fraction of vanadium in VO<sub>2</sub><sup>+</sup> and V<sub>2</sub>O<sub>4</sub><sup>2+</sup> phases while fixing bond distances and coordination numbers to their respective expected values and setting Debye–Waller parameters as shown in Table 4. This two-component refinement gave a vanadium fraction for vanadium with V<sub>2</sub>O<sub>4</sub><sup>2+</sup> structure of 36% ± 15% (Figure 8b), which is slightly below the maximum allowable dimer content (~50% of the V-atoms) estimated from Al–Al pair distributions in ZSM5 with Si/Al<sub>f,i</sub> of 13.4 (Section 3.2).

Simulated V-ZSM5 dimer structures (Figure 2) show a V–Al distance of 0.301 nm (0.284 nm for the monomer) and a V–V distance of 0.264 nm, but no second-shell V–V or V–Al distances are apparent in the measured radial structure functions. Crystalline oxides (e.g. V<sub>2</sub>O<sub>5</sub>) typically give a second-shell M–M (M = metal) feature (Figure 8a), but these are seldom observed in small oxide domains, because of weak scattering, nonidentical connectivity at nonuniform support anchoring sites, and possible destructive interference from multiple scattering paths,<sup>21,55</sup> as shown for Cu<sup>+</sup> cations exchanged onto H-ZSM5 (using sublimation of CuCl) with a Cu/Al<sub>f</sub> ratio of unity, in which only a Cu–O shell is detected.<sup>56</sup>

X-ray absorption fine structure spectra are consistent with coexisting monomers and dimers for V/Al<sub>f,f</sub> ratios near unity. Significant photon absorption by Si, Al, and O in ZSM5 led to signal-to-noise ratios inadequate for fine structure analysis for samples with smaller V/Al<sub>f,f</sub> ratios, for which we use Raman spectroscopy, as described in the next section, to measure vibrational modes in V<sub>x</sub>O<sub>2x</sub><sup>x+</sup> species as a function of V content.

**3.4. Raman Spectra of Grafted VO<sub>x</sub> Species.** Raman spectra for H-ZSM5 and V<sub>2</sub>O<sub>5</sub>, and for V-ZSM5 prepared by sublimation of VOCl<sub>3</sub> precursors onto H-ZSM5 are shown in Figure 9. Crystalline V<sub>2</sub>O<sub>5</sub> exposed to ambient air shows sharp bands at 997, 701, 529, 484, 408, 287, and 148 cm<sup>-1</sup>; these bands remained unchanged upon treatment at 623 K in flowing dry air. H-ZSM5 has framework modes at 300–500, 820, and 1190–1250 cm<sup>-1</sup>, arising from five- and ten-membered ring

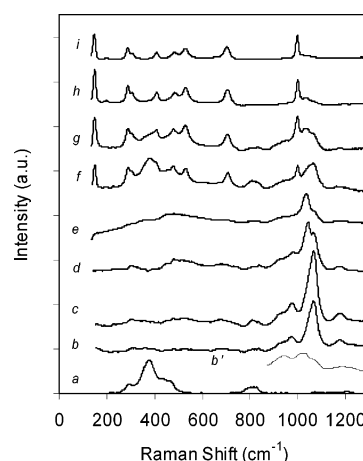


**Figure 9.** Raman spectra of H-ZSM5 and V-ZSM5 prepared from V<sub>2</sub>O<sub>5</sub> and VOCl<sub>3</sub>. (a) H-ZSM5; V-ZSM5 prepared using VOCl<sub>3</sub> with V/Al<sub>f,i</sub> ratios of (b) 0.2, (c) 0.4, (d) 0.65, and (e) 1; V-ZSM5 prepared using V<sub>2</sub>O<sub>5</sub> with V/Al<sub>f,i</sub> ratios of (f) 0.2, (g) 0.4, and (h) 1.0; (i) V<sub>2</sub>O<sub>5</sub>. Sample (b) was also hydrated using air saturated with H<sub>2</sub>O at 298 K in (b'). Zeolite samples were heated ex situ at 1023 K in dry air, then transferred to the Raman cell and dehydrated at 823 K in dry air before recording spectra at 298 K. The sample cell was rotated at 7 Hz to prevent local heating due to the laser. 9b–e represents difference spectra relative to H-ZSM5.

vibrations, T–O–T stretches, and T–O stretches; these bands are assigned here by analogy with modes reported for zeolite A.<sup>57</sup> Aluminum vanadate, AlVO<sub>4</sub>, has sharp bands at 1017, 988, and 949 cm<sup>-1</sup> for V=O in three distinct framework VO<sub>4</sub> tetrahedra,<sup>58</sup> a set of assignments confirmed by theory.<sup>59</sup>

V-ZSM5 samples (Figure 9) with 0.21 and 0.41 V/Al<sub>f,f</sub> ratios give strong broad features at 1065 cm<sup>-1</sup>; their intensities increased with increasing V content. Weaker bands at 980 and 1170 cm<sup>-1</sup> also became stronger with increasing V/Al<sub>f,f</sub> ratio. For V/Al<sub>f,f</sub> ratios above 0.5, an additional band appeared at 1044 cm<sup>-1</sup> with a shoulder at 1065 cm<sup>-1</sup>. The intensity of the 1044 cm<sup>-1</sup> band relative to the 1065 cm<sup>-1</sup> band is higher for the sample with the higher V/Al<sub>f,f</sub> ratio. Silanols were completely exchanged by V in the two samples with V/Al<sub>f,f</sub> > 0.5, as detected by infrared; thus, the band at 1044 cm<sup>-1</sup> is not related to V=O stretches in VO<sub>x</sub> exchanged at silanol sites. We tentatively assign this band to V<sub>2</sub>O<sub>4</sub><sup>2+</sup> dimers and propose that it appears first in samples with a V/Al<sub>f,f</sub> ratio of 0.65 and

**TABLE 5: Calculated Raman Shifts for V-ZSM5 Materials Based on VO<sub>2</sub><sup>+</sup> and V<sub>2</sub>O<sub>4</sub><sup>2+</sup>**

V <sup>5+</sup> Species	Raman shift (cm <sup>-1</sup> ) B3LYP/6-31 g(d)	Raman shift (cm <sup>-1</sup> ) S-VWN5/6-31 g(d)	band
VO <sub>2</sub> <sup>+</sup>	1076	1076	$\nu_s$ -V=O
	1072	1079	$\nu_{as}$ -V=O
	1020, 1000	1033	$O_f$ -V-O <sub>f</sub>
V <sub>2</sub> O <sub>4</sub> <sup>2+</sup>		1104, 1092, 1079	$\nu_s$ -V=O
		1060, 1038, 1033	$\nu_{as}$ -V=O
		766, 758, 734, 605	$\nu_s$ -O-V-O
		573, 567	$\nu_s$ -V-O <sub>f</sub> -Al

becomes more prevalent as the V<sup>5+</sup> content increases. As VO<sub>x</sub>(OH)<sub>2(2-x)</sub> forms (Scheme 1) during hydrolysis and becomes more abundant with increasing V/Al<sub>f,f</sub> ratio, these species are more likely to condense with another VO<sub>x</sub>(OH)<sub>2(2-x)</sub> to form a dimer, instead of forming a monomer by condensing with residual acidic OH groups.

The vibrational spectrum for VO<sub>2</sub><sup>+</sup> monomers (in Table 5) was calculated using DFT by determining optimal geometries and bond lengths, and calculating the frequencies for Raman-active modes. VO<sub>2</sub><sup>+</sup> monomers exhibit C<sub>2v</sub> symmetry (Figure 2) with two terminal V=O bonds (0.159 nm bonds) and two V-O<sub>f</sub> bonds (0.195 nm). These simulations indicate that VO<sub>2</sub><sup>+</sup> monomers exhibit two stretching modes for terminal V=O bonds at 1072 cm<sup>-1</sup> (antisymmetric) and 1076 cm<sup>-1</sup> (symmetric), which cannot be resolved in practice.<sup>60</sup> Framework vibrations from O<sub>f</sub>-V-O<sub>f</sub> bending stretches give bands at 1000 and 1020 cm<sup>-1</sup>, slightly higher but similar to those observed at 980 cm<sup>-1</sup>. The band at 1065 cm<sup>-1</sup> in the measured spectrum for all V-ZSM5 samples (prepared by VOCl<sub>3</sub> sublimation and hydrolysis) also resembles that predicted for terminal V=O stretches in VO<sub>2</sub><sup>+</sup> monomers (Figure 9).

The broad band centered at 1044 cm<sup>-1</sup> in samples with 0.65 and 1.1 V/Al<sub>f,f</sub> ratios is not present in the simulated spectrum for VO<sub>2</sub><sup>+</sup> species, suggesting that another V-oxo species coexists with VO<sub>2</sub><sup>+</sup> at high V/Al<sub>f,f</sub> ratios. The simulated spectrum for V<sub>2</sub>O<sub>4</sub><sup>2+</sup> dimers contains symmetric V=O stretches in the 1033–1104 cm<sup>-1</sup> frequency range.<sup>61</sup> The 980 cm<sup>-1</sup> band in samples with V/Al<sub>f,f</sub> < 0.5, attributed to O<sub>f</sub>-V-O<sub>f</sub> vibrations in VO<sub>2</sub><sup>+</sup>, also becomes weaker in the 0.65 and 1.1 V/Al<sub>f,f</sub> samples. A band centered near 500 cm<sup>-1</sup> appears in the spectra for samples with V/Al<sub>f,f</sub> > 0.5; this frequency is lower than predicted for V-O<sub>f</sub> stretches in V<sub>2</sub>O<sub>4</sub><sup>2+</sup> dimers (~570 cm<sup>-1</sup>); the broad nature of this band may reflect multiple dimer-surface connectivities as a result of nonuniform distributions of distances in Al-Al next-nearest neighbors required to anchor these dimers. Bridging V-O-V bonds, with predicted bands at 605–766 cm<sup>-1</sup> (Table 5), were not detected experimentally, but these are broad weak bands sometimes unobservable even in larger polyvanadate oligomers on mesoporous supports, such as Al<sub>2</sub>O<sub>3</sub>.<sup>43,62</sup> We tentatively assign the 1044 cm<sup>-1</sup> band in V-ZSM5 with high V/Al<sub>f,f</sub> ratios to V<sub>2</sub>O<sub>4</sub><sup>2+</sup> and conclude that dimers incipiently form V/Al<sub>f,f</sub> ratios near 0.5 and become more prevalent with increasing V content.

When species containing V=O bonds are well dispersed, their vibrational modes are perturbed by interactions with adsorbed molecules. Exposing dehydrated V-ZSM5 to air saturated with H<sub>2</sub>O at ambient temperature led to the disappearance of the 1044 and 1065 cm<sup>-1</sup> bands (e.g., the disappearance of the 1065 cm<sup>-1</sup> band for V/Al<sub>f,f</sub> = 0.21 in Figure 9, line *b*) and led to new weaker bands in the 950–1020 cm<sup>-1</sup> region that may represent hydrated V<sup>5+</sup>-oxo species shifted to lower energy; a subsequent treatment in dry air at 823 K restored the initial spectrum.

Species responsible for Raman bands at 1044 and 1065 cm<sup>-1</sup> are fully accessible to coordinate molecules and thus are highly dispersed.

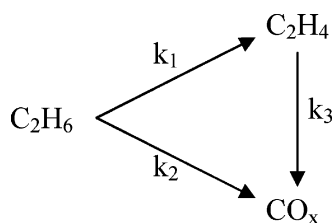
V<sub>2</sub>O<sub>5</sub> and AlVO<sub>4</sub> Raman bands were not detected in V-ZSM5 samples prepared by VOCl<sub>3</sub> sublimation, but crystalline V<sub>2</sub>O<sub>5</sub> was ubiquitous in samples prepared by treating physical mixtures of V<sub>2</sub>O<sub>5</sub> and H-ZSM5 in dry air at 973 K.<sup>63</sup> V<sub>2</sub>O<sub>5</sub>/ZSM5 physical mixtures (Figure 9) also gave bands at 1029 and 1060 cm<sup>-1</sup>, assigned to (SiO)<sub>3</sub>V=O<sup>15,58</sup> species at external surfaces or to small V<sub>2</sub>O<sub>5</sub> clusters; the band at 1029 cm<sup>-1</sup> was also present in V<sub>2</sub>O<sub>5</sub>/Al<sub>2</sub>O<sub>3</sub> samples prepared by impregnation with NH<sub>4</sub>VO<sub>3(aq)</sub>, and the 1060 cm<sup>-1</sup> band, for V=O stretches, was much weaker in V<sub>2</sub>O<sub>5</sub>/ZSM5 samples than in V-ZSM5 samples prepared by grafting VOCl<sub>3</sub>. Our results for physical mixtures differ from previous reports,<sup>14</sup> in which crystalline V<sub>2</sub>O<sub>5</sub> was not detected in UV-visible or X-ray absorption spectra of physical mixtures of V<sub>2</sub>O<sub>5</sub> and H-ZSM5 (V/Al = 0.4, Si/Al = 12) treated at 1073 K; these authors concluded that these protocols lead to the formation of (SiO)<sub>3</sub>-V=O species, probably via reaction with silanols prevalent at external surfaces. Our findings do not preclude the presence of such species, which may form, in addition to small V<sub>2</sub>O<sub>5</sub> clusters, on external surfaces and account for the Raman band at ~1030 cm<sup>-1</sup>. The presence or absence of residual V<sub>2</sub>O<sub>5</sub> after thermal treatment may depend on the V content and the external surface area of the different samples in these two studies.

V-ZSM5 (Table 1) prepared via aqueous exchange showed only one band (at 1070 cm<sup>-1</sup>) except for those for H-ZSM5. This band resembles that for V=O species in samples prepared by grafting of VOCl<sub>3</sub> (*b* and *c* in Figure 1), but is considerably weaker and accounts for <0.01 VO<sub>2</sub><sup>+</sup>/Al<sub>f</sub>. It appears that solvated VO<sub>2</sub><sup>+(aq)</sup> and V<sub>10</sub>O<sub>27</sub>(OH)<sup>5-</sup> ions, prevalent in solutions of ammonium metavanadate at pH values of 2.8–5, cannot enter the 10-ring channels in ZSM5. Similar restrictions during wet impregnation (Table 1) led to the predominant formation of VO<sub>x</sub> domains at external surfaces; these domains gave Raman bands (950 and 1050 cm<sup>-1</sup>) similar to those for V<sub>10</sub>O<sub>27</sub>(OH)<sup>5-</sup> ions in the impregnating solution and attributed to polyvanadate structures.<sup>64</sup>

A requirement for cations to interact with zeolite exchange sites is that precursors diffuse through spatially constrained voids. With crystalline precursors, diffusion can only occur by breaking M-O bonds to form smaller MO<sub>x</sub> species, a process that coincides with sublimation. Sublimation forms uncharged vapor species that penetrate small channels much more readily than hydrated metal-oxo oligomers in aqueous media. Exchange by sublimation of crystalline precursors requires that precursors be volatile at temperatures consistent with ZSM5 structural integrity (<1000 K) (e.g., MoO<sub>3(s)</sub> with a vapor pressure of 56 Pa at 973 K).<sup>65</sup> V<sub>2</sub>O<sub>5</sub>, unlike MoO<sub>3</sub>, has no detectable vapor pressure at 1000 K; therefore, it cannot access zeolite channels. In contrast, VOCl<sub>3(l)</sub> forms VOCl<sub>3(g)</sub> at very low temperatures (boiling point, 410 K), and these monomers enter zeolite channels without significant diffusional constraints.

**3.5. Ethane Oxidative Dehydrogenation on V-ZSM5.** C<sub>2</sub>H<sub>6</sub> ODH occurs via the pathways in Scheme 2 on supported VO<sub>x</sub> domains.<sup>66</sup> Primary dehydrogenation steps (reaction 1) occur in parallel with alkane combustion (reaction 2), while ethene formed in step 1 is combusted to CO and CO<sub>2</sub> (CO<sub>x</sub>) in step 3. H<sub>2</sub>O byproducts can inhibit all of these reactions.

The rates of primary dehydrogenation and combustion reactions were measured from rates of ethene and CO<sub>x</sub> formation, extrapolated to zero ethane conversion. Primary C<sub>2</sub>H<sub>6</sub> oxidative dehydrogenation rates and primary C<sub>2</sub>H<sub>4</sub> and CO<sub>x</sub>

SCHEME 2: C<sub>2</sub>H<sub>6</sub> Oxidative Dehydrogenation Pathway

**TABLE 6: Ethane Oxidative Dehydrogenation on V-ZSM5 Prepared Using VOCl<sub>3</sub> Precursors (673 K, 14 kPa C<sub>2</sub>H<sub>6</sub>, 1.7 kPa O<sub>2</sub>, balance He, C<sub>2</sub>H<sub>6</sub> conversions less than 2.5%)**

catalyst	V/Al <sub>f,i</sub>	primary C <sub>2</sub> H <sub>6</sub> dehydrogenation rate (10 <sup>-3</sup> mol s <sup>-1</sup> V <sup>-1</sup> )	rate constants	
			k <sub>2</sub> /k <sub>1</sub>	k <sub>3</sub> /k <sub>1</sub>
V-ZSM5	0 <sup>a</sup>	0.05 <sup>b</sup>	0.019	200
	0.2 <sup>a</sup>	0.93	0.58	100
	0.4 <sup>a</sup>	0.68	0.54	62
	0.65 <sup>a</sup>	1.3	0.70	44
	1.0 <sup>a</sup>	1.3	0.64	44
	0.36 <sup>c</sup>	0.037	0.25	-
	0.86 <sup>d</sup>	0.38	-	-
V <sub>2</sub> O <sub>5</sub> /Al <sub>2</sub> O <sub>3</sub> , 1.4 V/nm <sup>2</sup>	-	0.28 <sup>e</sup>	0.36	7
V <sub>2</sub> O <sub>5</sub> /Al <sub>2</sub> O <sub>3</sub> , 3.6 V/nm <sup>2</sup>	-	0.49 <sup>e</sup>	0.45	11
V <sub>2</sub> O <sub>5</sub> /Al <sub>2</sub> O <sub>3</sub> , 8 V/nm <sup>2</sup>	-	1.2 <sup>e</sup>	0.36	13

<sup>a</sup> Al<sub>f,i</sub> from <sup>27</sup>Al MAS NMR in H-ZSM5 before exchange. <sup>b</sup> Units of 10<sup>-3</sup> mol s<sup>-1</sup> Al<sub>f</sub><sup>-1</sup>. <sup>c</sup> 723 K, 0.2 g, 16.4 kPa C<sub>2</sub>H<sub>6</sub>, 2 kPa O<sub>2</sub>, prepared by impregnation, ref 16. <sup>d</sup> 673 K, 0.25 g, C<sub>2</sub>H<sub>6</sub>:O<sub>2</sub> = 2:1, 9 sccm, prepared by VOCl<sub>3</sub> exchange at 793 K, ref 17. <sup>e</sup> 663 K, ref 43.

selectivities are shown in Table 6 (673 K, 14 kPa C<sub>2</sub>H<sub>6</sub>, 1.7 kPa O<sub>2</sub>). Primary C<sub>2</sub>H<sub>4</sub> selectivities were 58–66% on all V-ZSM5 catalysts and k<sub>2</sub>/k<sub>1</sub> rate constant ratios increased slightly with increasing V/Al<sub>f,i</sub> ratio. Catalysts with V/Al<sub>f,i</sub> ratios of 0.65 and 1.1 (VOCl<sub>3</sub> precursors, hydrolyzed after exchange) gave similar rates (1.3 × 10<sup>-3</sup> mol s<sup>-1</sup> V<sup>-1</sup>) while the two samples with lower V/Al<sub>f,i</sub> ratio (0.21, 0.41) also gave similar, but slightly lower, rates (0.7–0.9 × 10<sup>-3</sup> mol s<sup>-1</sup> V<sup>-1</sup>). The k<sub>3</sub>/k<sub>1</sub> rate constant ratios decreased from 200 to 44 as the V/Al<sub>f,i</sub> ratio increased from 0 to 1, and then remained constant (44) at higher V contents. Primary C<sub>2</sub>H<sub>4</sub> formation rates were significantly higher than on V-ZSM5 samples prepared by impregnation (0.037 × 10<sup>-3</sup> mol s<sup>-1</sup> V<sup>-1</sup>) and tested at similar reactant pressures but significantly higher temperatures (723 K),<sup>16</sup> these impregnated samples contain poorly dispersed crystalline V<sub>2</sub>O<sub>5</sub>. V-ZSM5 prepared by VOCl<sub>3</sub> in the present study also showed much higher rates than H-ZSM5 exposed to VOCl<sub>3</sub> (V/Al = 0.86) at 793 K (0.38 × 10<sup>-3</sup> mol s<sup>-1</sup> V<sup>-1</sup>; 673 K, 67 kPa C<sub>2</sub>H<sub>6</sub>, 33 kPa O<sub>2</sub>).<sup>17</sup> These authors attributed the catalytic effects of V to site defects caused by V<sup>5+</sup> incorporation into zeolite framework; they also reported significant dealumination (40%)<sup>67</sup> as a result of the high-temperature VOCl<sub>3</sub> treatment at 793 K, which is apparently formed from VO<sub>x</sub>-Al<sub>2</sub>O<sub>3</sub> compounds. Mesoporous [V]-MCM-41, with vanadium in the framework, did not show detectable C<sub>2</sub>H<sub>6</sub> ODH rates below 723 K.<sup>68</sup>

H-ZSM5 shows very low activity for dehydrogenation and combustion of C<sub>2</sub>H<sub>6</sub> with high k<sub>3</sub>/k<sub>1</sub> ratios (~200) that decreased with increasing V/Al<sub>f,i</sub>, suggesting that acidic OH groups may catalyze C<sub>2</sub>H<sub>4</sub> oxidation, as proposed earlier.<sup>16,17,69</sup> Primary C<sub>2</sub>H<sub>6</sub> combustion is much faster on V-ZSM5 than on H-ZSM5. VO<sub>2</sub><sup>+</sup> and V<sub>2</sub>O<sub>4</sub><sup>2+</sup> surface species that are active for combustion should also increase the rate of combustion of C<sub>2</sub>H<sub>4</sub>, which is more reactive than C<sub>2</sub>H<sub>6</sub>. As can be seen in Table 6, the k<sub>3</sub>/k<sub>1</sub> ratio

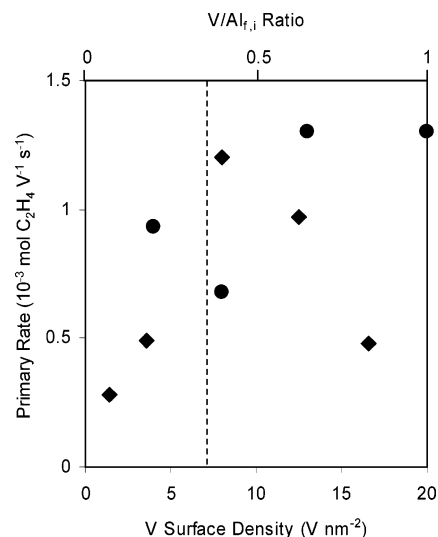


**Figure 10.** Primary C<sub>2</sub>H<sub>4</sub> formation rate as a function of V/Al<sub>f,i</sub> ratio for V-ZSM5 (circles, 673 K, 14 kPa C<sub>2</sub>H<sub>6</sub>, 1.7 kPa O<sub>2</sub>) or vanadia surface density on VO<sub>x</sub>/Al<sub>2</sub>O<sub>3</sub> (diamonds, 663 K, 14 kPa C<sub>2</sub>H<sub>6</sub>, 1.7 kPa O<sub>2</sub>). The broken line indicates the maximum polyvanadate surface coverage for VO<sub>x</sub>/Al<sub>2</sub>O<sub>3</sub> from ref 43.

decreases monotonically up to V/Al<sub>f,i</sub> = 0.65, but levels off at 44, suggesting that the decrease in k<sub>3</sub>/k<sub>1</sub> from replacement of H<sup>+</sup> is somewhat compensated by C<sub>2</sub>H<sub>4</sub> oxidation on VO<sub>2</sub><sup>+</sup> and V<sub>2</sub>O<sub>4</sub><sup>2+</sup>.

The observed trends in V-ZSM5 with V content resemble those reported on Al<sub>2</sub>O<sub>3</sub>-supported VO<sub>x</sub> domains prepared by impregnation.<sup>43</sup> At low surface densities, monomeric VO<sub>x</sub> species prevail and show very low ODH turnover rates (Table 6, 0.3 × 10<sup>-3</sup> mol V<sup>-1</sup> s<sup>-1</sup>). Turnover rates increased with VO<sub>x</sub> surface density up to polyvanadate monolayer values (~7 V/nm<sup>2</sup>, Figure 10 and Table 6), and then decreased as V<sub>2</sub>O<sub>5</sub> with inaccessible V centers formed. Dispersed two-dimensional polyvanadates are the predominant species near monolayer coverages, and they are significantly more active than monovanadates, as a result of their more reducible nature (in H<sub>2</sub> and during rate-determining C–H activation in ODH catalytic cycles) and greater ability to delocalize electron density during reduction events.<sup>70</sup> ODH turnover rates on V-ZSM5 with V/Al<sub>f,i</sub> ratios above 0.5 are ~50% higher than on the two samples with lower V content, which contain exclusively VO<sub>2</sub><sup>+</sup> monomers. Larger V<sup>5+</sup> domains, such as in polyvanadates on Al<sub>2</sub>O<sub>3</sub> or V<sub>2</sub>O<sub>4</sub><sup>2+</sup> dimers on H-ZSM5, start to form as VO<sub>x</sub> surface density increases; these oligomers contain both terminal and bridging O-atoms, whereas monovanadates only contain terminal oxygen.<sup>43,70</sup> The V–O–Al bond, which is expected to be more strained in dimers than in a monomers, a result of vicinal Al atom rearrangements when anchoring V<sub>2</sub>O<sub>4</sub><sup>2+</sup>, may also contribute to their enhanced activity.<sup>69</sup> The observed catalytic activity of V-ZSM5 for C<sub>2</sub>H<sub>6</sub> ODH, which is higher than in V-ZSM5 prepared by impregnation methods, is a result of highly disperse VO<sub>2</sub><sup>+</sup> and V<sub>2</sub>O<sub>4</sub><sup>2+</sup> species deduced by complementary characterization techniques and studies of catalytic trends with V/Al<sub>f,i</sub> ratios.

## Conclusions

VO<sub>2</sub><sup>+</sup> cations were formed on H-ZSM5 with V/Al<sub>f,i</sub> ≤ 0.5 by vapor exchange of VOCl<sub>3</sub> with hydroxyl species. The formation of VO<sub>2</sub><sup>+</sup> proceeds by the surface reaction of chloride ligands in VOCl<sub>3</sub> with Si–OH–Al, followed by hydrolysis of residual chloride. Complete exchange with Si–OH–Al can be

achieved with a constant exchange stoichiometry for V/Al<sub>f,i</sub> ≤ 1; however, a second species attributed to V<sub>2</sub>O<sub>4</sub><sup>2+</sup> dimers begins to form at V/Al<sub>f,i</sub> ratios above 0.5 as shown using Raman and X-ray absorption fine structure spectra. V<sub>2</sub>O<sub>5</sub> was not detected in these materials at any loading using Raman and X-ray absorption spectra. In contrast, V-ZSM5 prepared by impregnation and V<sub>2</sub>O<sub>5</sub>/H-ZSM5 physical mixtures treated in dry air at 973–1073 K lead to polymeric VO<sub>x</sub> clusters at external surfaces.

Raman spectra of V-ZSM5 prepared from VOCl<sub>3</sub> had a band at 1065 cm<sup>-1</sup> that was assigned to V=O using theoretical stretching frequencies from DFT. Exchanged VO<sub>2</sub><sup>+</sup> resembles the vanadate ion coordinated to a framework Al atom, [Al<sub>f</sub>]VO<sub>4</sub><sup>-</sup>, and is isostructural with KClO<sub>4</sub> and NaReO<sub>4</sub>. Vanadium K-edge X-ray absorption spectra (EXAFS) confirmed the presence of V in the +5 oxidation state. The extended X-ray absorption fine structure spectrum of V-ZSM5 was consistent with a mixture of VO<sub>2</sub><sup>+</sup> and V<sub>2</sub>O<sub>4</sub><sup>2+</sup> species at 1.1 V/Al<sub>f,f</sub>.

V-ZSM5 materials were active for the oxidative dehydrogenation of C<sub>2</sub>H<sub>6</sub> at 673 K. Primary ODH rates increased with V loading, a result that was attributed to the formation of dimers above V/Al<sub>f,f</sub> ratios of 0.5. Acidic H<sup>+</sup> in H-ZSM5 was found to be active for the combustion of C<sub>2</sub>H<sub>4</sub>; however, exchange with V<sup>5+</sup> decreased k<sub>3</sub>/k<sub>1</sub> ratios from 200 in H-ZSM5 to 44 in V-ZSM5 with 1.1 V/Al<sub>f,f</sub>.

**Acknowledgment.** The authors acknowledge partial financial support for the studies reported here by BP as part of the Berkeley-Caltech Methane Conversion Cooperative Program under the technical stewardship of Dr. Theo Fleisch (BP). H.L. acknowledges with thanks the financial support of the Ford Corporation through the Ford Catalysis Fellowship administered by the Berkeley Catalysis Center. X-ray absorption data were collected at the Stanford Synchrotron Research Laboratory, a national user facility operated by Stanford University on behalf of the U.S. Department of Energy, Office of Basic Energy Sciences. Drs. David Dixon, Kathy Durken and Aditya Bhan are also acknowledged for their valuable advice about the use of molecular simulations.

## References and Notes

- Veltri, M.; De Luca, P.; Nagy, J. B.; Nastro, A. *Thermochim. Acta* **2004**, *420*, 145.
- Kornatowski, J.; Sychev, M.; Kuzenkov, S.; Strnadová, K.; Pilz, W.; Kassner, D.; Pieper, G.; Baur, W. H. *J. Chem. Soc., Faraday Trans.* **1995**, *91*, 2217.
- Kornatowski, J.; Wichterlová, B.; Jirkovský, J.; Löffler, E.; Pilz, W. *J. Chem. Soc., Faraday Trans.* **1996**, *92*, 1067.
- Sen, T.; Rajamohanon, S.; Ganapathy, S.; Sivasanker, S. *J. Catal.* **1996**, *163*, 354.
- Tuel, A.; Taàrit, Y. B. *Zeolites* **1994**, *14*, 18.
- Centi, G.; Perathoner, S.; Trifiró, F.; Aboukais, A.; Aïssi, C. F.; Guelton, M. *J. Phys. Chem.* **1992**, *96*, 2617.
- Adams, R. C.; Xu, L.; Moller, K.; Bein, T.; Delgass, W. N. *Catal. Today* **1997**, *33*, 263.
- Dzwigaj, S.; Che, M. *J. Phys. Chem. B* **2005**, *109*, 22167.
- Dzwigaj, S.; Matsuoka, M.; Anpo, M.; Che, M. *Catal. Lett.* **2001**, *72*, 211.
- Dzwigaj, S.; Peltre, M. J.; Massiani, P.; Davidson, A.; Che, M.; Sen, T.; Sivasanker, S. *Chem. Commun.* **1998**, 87.
- Weckhuysen, B. M.; Wang, D. J.; Rosynek, M. P.; Lunsford, J. H. *J. Catal.* **1998**, *175*, 338.
- Huang, M.; Shan, S.; Yuan, C.; Li, Y.; Wang, Q. *Zeolites* **1990**, *10*, 772.
- Petráš, M.; Wichterlová, B. *J. Phys. Chem.* **1992**, *96*, 1805.
- Zhang, S. G.; Higashimoto, S.; Yamashita, H.; Anpo, M. *J. Phys. Chem. B* **1998**, *102*, 5590.
- Whittington, B. I.; Anderson, J. R. *J. Phys. Chem.* **1991**, *95*, 3306.
- Kao, C.-Y.; Juang, K.-T.; Wan, B.-Z. *Ind. Eng. Chem. Res.* **1994**, *33*, 2066.
- Chang, Y.-F.; Somorjai, G. A.; Heinemann, H. *J. Catal.* **1995**, *154*, 24.
- Lacheen, H. S.; Iglesia, E. *Phys. Chem. Chem. Phys.* **2005**, *7*, 538.
- Baes, C. F.; Mesmer, P. E. *The Hydrolysis of Cations*; John Wiley and Sons: New York, 1976; p 210.
- Hall, W. K.; Leftin, H.; Cheselke, F.; O'Reilly, D. E. *J. Catal.* **1963**, *2*, 506.
- Li, W.; Meitzner, G. D.; Borry, R. W.; Iglesia, E. *J. Catal.* **2000**, *191*, 373.
- Q<sup>n</sup>(nAl) represents a Si atom with nAl neighbors.
- Engelhardt, G.; Lohse, U.; Lippmaa, E.; Tarmak, M.; Mägi, M. Z. *Anorg. Allg. Chem.* **1981**, *482*, 49.
- Ressler, T. WinXAS; Version 2.1 ed.; T. Ressler.
- Newville, M.; Ravel, B.; Haskell, D.; Rehr, J. J.; Stern, A.; Yacoby, Y. *Physica B* **1995**, *208*, 154.
- Vaarkamp, M.; Linders, J. C.; Koningsberger, D. C. *Physica B* **1995**, *208 & 209*, 159.
- Lytle, F. W.; Sayers, D. E.; Moore, E. B. *Appl. Phys. Lett.* **1975**, *24*, 45.
- Kampers, F. W. H.; Engelen, C. W. R.; van Hooff, J. H. C.; Koningsberger, D. C. *J. Phys. Chem.* **1990**, *94*, 8574.
- Rehr, J. J.; Albers, R. C.; Zabinsky, S. I. *Phys. Rev. Lett.* **1992**, *69*, 3397.
- Ravel, B. *J. Synchrotron Radiat.* **2001**, *8*, 314.
- Frisch, M. J.; Trucks, G. W.; Schlegel, H. B.; Scuseria, G. E.; Robb, M. A.; Cheeseman, J. R.; Montgomery, J. A., Jr.; Vreven, T.; Kudin, K. N.; Burant, J. C.; Millam, J. M.; Iyengar, S. S.; Tomasi, J.; Barone, V.; Mennucci, B.; Cossi, M.; Scalmani, G.; Rega, N.; Petersson, G. A.; Nakatsuji, H.; Hada, M.; Ehara, M.; Toyota, K.; Fukuda, R.; Hasegawa, J.; Ishida, M.; Nakajima, T.; Honda, Y.; Kitao, O.; Nakai, H.; Klene, M.; Li, X.; Knox, J. E.; Hratchian, H. P.; Cross, J. B.; Bakken, V.; Adamo, C.; Jaramillo, J.; Gomperts, R.; Stratmann, R. E.; Yazyev, O.; Austin, A. J.; Cammi, R.; Pomelli, C.; Ochterski, J. W.; Ayala, P. Y.; Morokuma, K.; Voth, G. A.; Salvador, P.; Dannenberg, J. J.; Zakrzewski, V. G.; Dapprich, S.; Daniels, A. D.; Strain, M. C.; Farkas, O.; Malick, D. K.; Rabuck, A. D.; Raghavachari, K.; Foresman, J. B.; Ortiz, J. V.; Cui, Q.; Baboul, A. G.; Clifford, S.; Cioslowski, J.; Stefanov, B. B.; Liu, G.; Liashenko, A.; Piskorz, P.; Komaromi, I.; Martin, R. L.; Fox, D. J.; Keith, T.; Al-Laham, M. A.; Peng, C. Y.; Nanayakkara, A.; Challacombe, M.; Gill, P. M. W.; Johnson, B.; Chen, W.; Wong, M. W.; Gonzalez, C.; Pople, J. A. *Gaussian 03*, revision C.02; Gaussian, Inc.: Wallingford, CT, 2004.
- Slater, J. C. *Quantum Theory of Molecules and Solids*; McGraw-Hill: New York, 1974; Vol. 4.
- Vosko, S. J.; Wilk, L.; Nusair, M. *Can. J. Phys.* **1980**, *58*, 1200.
- Lee, C.; Yang, W.; Parr, R. G. *Phys. Rev. B* **1988**, *37*, 785.
- Becke, A. D. *J. Chem. Phys.* **1993**, *98*, 5648.
- Hariharan, P. C.; Pople, J. A. **1973**, *28*, 213.
- van Koningsveld, H.; van Bekkum, H.; Jansen, J. C. *Acta Crystallogr. B: Struct. Sci.* **1987**, *127*.
- A T-site denotes a Si or Al in a framework ZSM5 position. There are 24 different T-sites in calcined H-ZSM5.
- Florián, J.; Johnson, B. G. *J. Phys. Chem.* **1994**, *98*, 3681.
- Dunlap, B. I.; Andzelm, J. *Phys. Rev. A* **1992**, *45*, 81.
- Wong, M. W. *Chem. Phys. Lett.* **1996**, *256*, 391.
- Fielicke, A.; Mitric, R.; Meijer, G.; Bonacic-Koutecky, V. B.; von Helden, G. *J. Am. Chem. Soc.* **2003**, *125*, 15716.
- Argyle, M. D.; Chen, K.; Bell, A. T.; Iglesia, E. *J. Catal.* **2002**, *208*, 139.
- Biscardi, J. A.; Meijer, G.; Iglesia, E. *J. Catal.* **1998**, *179*, 192.
- Muller, M.; Harvey, G.; Prins, R. *Microporous Mesoporous Mater.* **2000**, *34*, 281.
- Li, W.; Yu, S. Y.; Meitzner, G. D.; Iglesia, E. *J. Phys. Chem. B* **2001**, *1005*, 1176.
- Unpublished experiments of D<sub>2</sub> titration in zeolites with high silanol content found that OH bands at 3740 and 3600 cm<sup>-1</sup> shifted to 2750 and 2640 cm<sup>-1</sup>.
- Kazansky, V. B.; Serykh, A. I.; Semmer-Herledan, V.; Fraissard, J. *Phys. Chem. Chem. Phys.* **2003**, *5*, 966.
- Rice, G. L.; Scott, S. L. *Langmuir* **1997**, *12*, 111545.
- Engelhardt, G.; Michel, D. *High-Resolution Solid-State NMR of Silicates and Zeolites*; Wiley: Chichester, 1987.
- Rice, M. J.; Chakraborty, A. K.; Bell, A. T. *J. Catal.* **1999**, *186*, 222.
- Vanadium concentrations below V/Al<sub>f</sub> = 1 were inadequate to obtain EXAFS due to competing Al, Si, and O absorption.
- Lee, P. A.; Beni, G. *Phys. Rev. B* **1977**, *15*, 2862.
- Byström, A.; Wilhelmi, K.-A.; Brotzen, O. *Acta Chem. Scand.* **1950**, *4*, 1119.

- (55) Deguns, E. W.; Taha, Z.; Meitzner, G. D.; Scott, S. L. *J. Phys. Chem. B* **2005**, *109*, 5005.
- (56) Lamberti, C.; Bordiga, S.; Salvalaggio, M.; Spoto, G.; Zecchina, A.; Geobaldo, F.; Vlaic, G.; Bellatreccia, M. *J. Phys. Chem. B* **1997**, *101*, 344.
- (57) Dutta, P. K.; Del Barco, B. *J. Phys. Chem.* **1988**, *92*, 354.
- (58) Hardcastle, F. D.; Wachs, I. E. *J. Phys. Chem.* **1991**, *95*, 5031.
- (59) Brázdová, V.; Ganduglia-Pirovano, M. V.; Sauer, J. *J. Phys. Chem. B* **2005**, *109*, 394.
- (60) V=O frequencies in fully relaxed VO<sub>2</sub>(OH)<sub>2</sub>Al(OH)<sub>2</sub> were 1067 (antisymmetric) and 1070 cm<sup>-1</sup> (symmetric).
- (61) Private communication with Dave Dixon, 113b Shelby Hall, University of Alabama, Department Chemistry, Tuscaloosa, AL 35487 (dadixon@bama.ua.edu).
- (62) Weckhuysen, B. M.; Keller, D. E. *Catal. Today* **2003**, *78*, 25.
- (63) V<sub>2</sub>O<sub>5</sub> bands also persisted after treatment at 1073 K for 2 h in dry air.
- (64) Griffith, W. P.; Wickins, T. D. *J. Chem. Soc. A—Inorg. Phys. Theor.* **1966**, *8*, 1087.
- (65) *Thermochemical Properties of Inorganic Substances*; 2nd ed.; Knacke, O., Kubaschewski, O., Hesselmann, K., Eds.; Springer-Verlag: Berlin, 1991.
- (66) Argyle, M. D.; Chen, K.; Bell, A. T.; Iglesia, E. *J. Phys. Chem. B* **2002**, *106*, 5421.
- (67) Chang, Y.-F.; Somorjai, G. A.; Heinemann, H. *Appl. Catal. A: Gen.* **1993**, *96*, 305.
- (68) Zhang, Q.; Wang, Y.; Ohishi, Y.; Shishido, T.; Takehira, K. *J. Catal.* **2001**, *202*, 308.
- (69) Bañaras, M. A. *Catal. Today* **1999**, *51*, 319.
- (70) Chen, K.; Bell, A. T.; Iglesia, E. *J. Catal.* **2002**, *209*, 35.